REPORT DOCUMENTATION PAGE

AFRL-SR-BL-TR-01-

0336

1. AGENCY USE ONLY *(Leave blank)*	2. REPORT DATE	3. REPORT TYPE AND DATES COVERED
		FINAL 15 JUN 95 TO 14 JUN 98

4. TITLE AND SUBTITLE
(AASERT -95) BAND OFFSETS AND INFRARED DETECTOR APPLICATIONS OF (SI1-XY GEXCY) ALLOYS)

5. FUNDING NUMBERS
61103D
3484/TS

6. AUTHOR(S)
PROFESSOR JAMES C. STURM

7. PERFORMING ORGANIZATION NAME(S) AND ADDRESS(ES)
PRINCETON UNIVERSITY
DEPARTMENT OF ELECTRICAL ENGINEERING
CENTER FOR PHOTONICS 7 OPTOELECTRONIC MATERIALS (POEM)
PRINCETON, NJ 08544

8. PERFORMING ORGANIZATION REPORT NUMBER

F49620-95-1-0438

9. SPONSORING/MONITORING AGENCY NAME(S) AND ADDRESS(ES)
AIR FORCE OF SCIENTIFIC RESEARCH
801 NORTH RANDOLPH ST RM732
ARLINGTON, VA 22203-1977

10. SPONSORING/MONITORING AGENCY REPORT NUMBER

11. SUPPLEMENTARY NOTES
APPROVED FOR PUBLIC RELEASE, DISTRIBUTION UNLIMITED

12a. DISTRIBUTION AVAILABILITY STATEMENT

AIR FORCE OFFICE OF SCIENTIFIC RESEARCH (AFOSR)
NOTICE OF TRANSMITTAL DTIC. THIS TECHNICAL REPORT HAS BEEN REVIEWED AND IS APPROVED FOR PUBLIC RELEASE LAW AFR 190-12 DISTRIBUTION IS UNLIMITED.

13. ABSTRACT *(Maximum 200 words)*
The band offest of Si1xyGexCy/Si in pseudomorphic structures grown on Si(100) subr. ates has been experimentally measured by using both electrical (capacitance-voltage) measurements and by making heterojunction internal photoemission (HIP) infrared detector. By measuring the cutoff wavelength of the IR detectors, one makes a direct measurement of the valence band offset. The two methods are in good agreement with each other, and find that as carbon is added to these structures, pseudomorphic to Si(100) substrates, the valence band in the SiGeC rises at a rate of 26 me V/%C. Thus the valence band offset to Si decreases at the same rate. There is no detectable change on the position of the conduction band a C is added.

20010612 030

14. SUBJECT TERMS			15. NUMBER OF PAGES
			16. PRICE CODE

17. SECURITY CLASSIFICATION OF REPORT	18. SECURITY CLASSIFICATION OF THIS PAGE	19. SECURITY CLASSIFICATION OF ABSTRACT	20. LIMITATION OF ABSTRACT
UNCLASSIFIED	UNCLASSIFIED	UNCLASSIFIED	UL

Final Report

AFOSR Contract No: F49620-95-1-0438 (AASERT-95)

Band Offsets and Infrared Detector Applications of $Si_{1-x-y}Ge_xC_y$ Alloys

Report period: June 1995 - June 1998

Report date: March, 2001

Prof. James C. Sturm

Department of Electrical Engineering

Center for Photonics and Optoelectronic Materials (POEM)

Princeton University

Princeton, NJ 08544

609-258-5610, fax: 609-258-1954, sturm@ee.princeton.edu

Summary:

The band offset of $Si_{1-x-y}Ge_xC_y$/Si in pseudomorphic structures grown on Si(100) substrates has been experimentally measured by using both electrical (capacitance-voltage) measurements and by making heterojunction internal photoemission (HIP) infrared detectors. By measuring the cutoff wavelength of the IR detectors, one makes a direct measurement of the valence band offset. The two methods are in good agreement with each other, and find that as carbon is added to these structures, pseudomorphic to Si(100) substrates, the valence band in the SiGeC rises at a rate of ~26 meV/%C. Thus the valence band offset to Si decreases at the same rate. There is no detectable change on the position of the conduction band as C is added.

Introduction

$Si_{1-x-y}Ge_xC_y$/Si heterojunctions are of great interest for extending the properties of silicon-based devices. The advantage of using strained $Si_{1-x}Ge_x$/Si heterostructures results from the flexibility in bandgap engineering by controlling the amount of incorporated Ge into Si matrix. However, due to the 4% larger lattice constant of Ge than that of Si, the strain involved in $Si_{1-x}Ge_x$ prevents one from growing a thick $Si_{1-x}Ge_x$ layer on a Si substrate without introducing misfit dislocations. Recently $Si_{1-x-y}Ge_xC_y$ has attracted strong interest due to the ability of substitutional carbon to compensate the strain caused by Ge atoms, with 1% substitutional carbon compensating the strain caused by 8-10 % Ge [1-6]. Up to 2.5% substitutional carbon in Si and $Si_{1-x}Ge_x$ have been reported, even though the equilibrium solubility of carbon in Si is only 0.01% [7,8].

Of specific interest for this report is the ability of Si-based heterostructures to be used for infrared detection to 10 micron wavelengths and beyond. For example, the well-known PtSi (platinum silicide) on silicon technology typically cuts off at ~5 microns wavelengths due to the barrier height between the fermi level in PtSi and the valence band of silicon [9]. The effect of adding Ge to create a strained $Si_{1-x}Ge_x$ alloy commensurate to the Si(100) substrate is well known to be to raise the level of the valence band which in turn will lower the barrier height for holes to cross from the silicide into the semiconductor (Fig 1) . This raises the cutoff wavelength of the detector [10]. This concept has been demonstrated out to 10 microns cutoff wavelength [11,12].

For the large amounts of Ge required to substantially lower the barrier height, there is a critical thickness to which the $Si_{1-x}Ge_x$ layer can be grown with a low number of defects. Photoluminescence (PL) studies and electrical measurements on pseudomorphic compressively strained $Si_{1-x-y}Ge_xC_y$ on Si (100) show that 1% C increases the bandgap of

$Si_{1-x-y}Ge_xC_y$ alloys by 21~26 meV [13-16]. Given only a slight increase of bandgap by C incorporation, a strained $Si_{1-x-y}Ge_xC_y$ layer would have a smaller bandgap than that of an equally strained $Si_{1-x}Ge_x$ layer [13] (Fig. 2). Alternatively, for the same band gap reduction from Si, pseudomorphic $Si_{1-x-y}Ge_xC_y$ would have less strain and a higher critical thickness than $Si_{1-x}Ge_x$. This sets the clear motivation for the study of the SiGeC system for infrared detector engineering. Other application would include quantum-well infrared detectors (QUIP's) and heterojunction internal photoemission (HIP) based detectors.

This report describes the measurement of the Si/SiGeC valence band offset as a function of C content by both electrical and optical methods. Infrared detection is demonstrated using this material system in a HIP configuration -- and indeed the cutoff wavelength of these devices is one measurement of the valence band offset.

II. Measurement of the SiGeC/Si Valence Band Offset

II.A. Sample Growth and Preparation

The samples in this study contain 39% Ge and up to 2.5% substitutional carbon and were grown by Rapid Thermal Chemical Vapor Deposition RTCVD as in reference 7. They contain a p^+ Si buffer for substrate contact, followed by 0.2 μm p^- Si, 2 nm undoped $Si_{1-x-y}Ge_xC_y$ spacer and 18 nm p^+ $Si_{1-x-y}Ge_xC_y$ (~ 10^{19}/cm^3). Finally, a 20 nm heavily doped (~ 10^{20}/cm^3) Si layer was grown for a top contact. It is noted that the doping concentration in p+ $Si_{1-x-y}Ge_xC_y$ is not expected to induce bandgap narrowing since we reported in capacitance-voltage measurement that no effect on ΔE_V is observed with varying doping concentrations [7]. Ge content was determined by X-ray diffraction and the number is consistent with results by SIMS and photoluminescence studies. Substitutional C fractions were measured by X-ray diffraction, assuming 8.3 Ge/C strain compensation ratio. For the rest of this paper, all carbon levels refer to the substitutional levels measured by this method.

Device were fabricated by a simple mesa etching in CF_4/O_2 plasma and Al metallization by lift-off.

Figure 3 shows the (400) X-ray diffraction (XRD) performed on the strained $Si_{1-x-y}Ge_xC_y$ layers with 39.5% Ge and various C concentrations. The concentration of Ge was obtained by measuring the no-carbon XRD peak relative to that of Si substrate. This value is consistent with the Ge concentration obtained by PL measurements. As C is added, the peak starts shifting toward the Si peak, indicating decreased lattice constant, i.e., reduced strain. Broad peaks of $Si_{1-x-y}Ge_xC_y$ are indication of Scherer broadening in the thin films which becomes more prominent as more C is added, qualitatively consistent with an assumed reduction in growth rate as C is added. High resolution transmission electron microscopy (HRTEM) performed on the $Si_{0.9485}Ge_{0.0395}C_{0.012}$ sample (measured thickness ~ 21nm) shows good interface quality and no evidence of dislocations or SiC precipitates. The thickness of the $Si_{0.9485}Ge_{0.0395}C_{0.012}$ layer is 21 nm. Assuming that the Ge content was unchanged by the addition of methylsilane at constant germane flow, the substitutional C content was quantified by measuring the relative shift of the XRD peak of $Si_{1-x-y}Ge_xC_y$ layers with respect to that of $Si_{1-x}Ge_x$, assuming a Ge:C strain compensation ratio of 8.3 [17] . A substitutional C level of up to 2.5% was measured. To the best knowledge of the authors, this is the highest single crystal value reported to date by Chemical Vapor Deposition (CVD).

Good rectifying characteristics were observed at low temperatures (~ 77K), indicating a significant valence band offset between p^+ $Si_{1-x-y}Ge_xC_y$ / p^- Si. Samples were further cooled down to ~ 4 K to minimize thermionic leakage current for infrared photocurrent measurements and a good ohmic contact was still observed. Optical absorption measurements were performed at 4K using a calibrated glowbar IR source, a spectrometer and a phase sensitive detection.

Although it is generally agreed that 1% carbon increases bandgap by 21~26 meV, it is still under debate regarding how this bandgap increase is allocated in the conduction and valence band alignments of $Si_{1-x-y}Ge_xC_y$ to the Si substrate. Generally, the valence band offset of $Si_{1-x-y}Ge_xC_y$ /Si has been studied. A temperature-dependent leakage current study on p^+ $Si_{1-x-y}Ge_xC_y$ / p^- Si unipolar diodes indicated that carbon decreased the valence band offset (ΔE_v) of the resulting $Si_{1-x-y}Ge_xC_y$ /Si heterostructure [18]. However, no accurate quantitative number was extracted due to scatter in data among devices caused by strong dependence of leakage current on local defects.

Under reverse bias ($V_{SiGeC} > V_{Si}$), the valence band offset (ΔE_v) between $Si_{1-x-y}Ge_xC_y$ and Si blocks hole current from p^+ $Si_{1-x-y}Ge_xC_y$, so that the device rectifies at low temperature. Shown in figure 4 is the reverse-biased valence band diagram (with V_{SiGeC} - V_{Si} = 0.3 V). $E_{F(SiGeC)}$ is the position of Fermi level relative to the valence band of $Si_{1-x-y}Ge_xC_y$, V_{bi} is the built-in voltage of the junction, $E_{F(Si)}$ is the position of the valence band of Si relative to the Fermi level. In theory, ΔE_v may be measured by temperature dependence of the leakage current which is ideally from themionic emission of holes from $Si_{1-x-y}Ge_xC_y$ into Si. However, the leakage current for the entire device can be easily dominated by non-ideal sources at a few local defects, edge effects, depletion region generation, etc. Therefore, to measure the band offset, we used a capacitance-voltage technique, which is less affected by local defects and leakage currents. We found that capacitance-voltage measurements were more repeatable from sample to sample and had far less scatter among devices on the same wafer than leakage current measurements [18]. The capacitances were measured as a function of reverse bias at 100 K with a AC frequency from 10 KHz to 4 MHz, and an AC amplitude at 25-50 mV. Much like a Schottky barrier or a one-sided pn junction, the capacitance per unit area C is given by [19]

$$C^{-2} = 2 (V_{bi}-V)/(q\varepsilon N_A) \tag{1}$$

where V is the DC bias and N_A is the doping concentration on the Si side of the heterojunction. By plotting $1/C^2$ vs. applied DC voltage, the doping level on the p⁻ Si side as well as built-in potential of the junction can be obtained. Figure 5 shows the capacitance-voltage characteristics of the samples containing 39.5% Ge and various C contents. The $1/C^2$-V data points are linear over the range of applied voltages, and the extracted Si doping concentrations are in the range of $10^{17}/cm^3$. The variation of the doping level among samples was due to the variation in the doping level of bottom contact layers and background doping. Spreading resistance measurement was performed on one of the samples and the measured doping concentration is consistent with that obtained by $1/C^2$-V data. It is also noted that the slope and intercept were not affected by AC amplitude used in this study (25-50 mV), and the data shown in figure 5 were measured with AC amplitude equal to 30 mV. Based on the doping level, we calculated $E_{F(Si)}$ at 100K in each sample. The extrapolated built-in voltages decrease as more C is added. $E_{F(SiGeC)}$ was obtained by a straightforward calculation from the doping concentrations in the $Si_{1-x-y}Ge_xC_y$, which were measured by SIMS on similarly grown layers, and by assuming an effective mass independent of C level. SIMS measurements show that the boron incorporation in $Si_{1-x-y}Ge_xC_y$ does not depend on the C level for a given diborane flow.

ΔE_v was calculated by combining qV_{bi}, $E_{F(SiGeC)}$ and $E_{F(Si)}$, as illustrated in Figure 4. There is a consistent decrease in the valence band offset of $Si_{1-x-y}Ge_xC_y$/Si as C is added (see Figure 6) . Growth temperature, dopings and Ge level have no significant effect on the effect of C on ΔE_v. The observed dependence for the three samples plotted are 25±1 meV/%C, 20±1 meV/%C, and 26±3 meV/%C for lines fitted to data points up to 1.3%. For the one series with 2.5%C, the slope is somewhat larger from 1.3% to 2.5% C (37±2 meV/%C). It is not known if this change in slope is significant (e.g. bowing in curve of bandgap vs. lattice constant) or not. In any case, the rest of the report focuses on C concentrations under 1.5% as these are of the greatest technological relevance. We also found that the *absolute* ΔE_v measured by the capacitance-voltage technique varied slightly with different AC frequencies (within 15 meV from 10 KHz to 1 MHz). However, the

6

change of ΔE_V with C at a given frequency was negligibly influenced by the measurement frequency (< 4 meV/%C). Comparison to the total bandgap change of 21-26 meV (measured up to 1%C) indicates that all of the change in bandgap as C is added to strained $Si_{1-x-y}Ge_xC_y$ is accommodated in the valence band within experimental results.

II.C. Band Offset Measurement by Heterojunction Internal Photoemission

To confirm the above electrical measurements based on the C-V technique, it is desired to have a direct optical measurement on the band offset in $Si_{1-x-y}Ge_xC_y$ /Si (100) heterostructures. We now describe such a measurement by heterojunction internal photoemission (HIP) on the valence band offset of p^+ $Si_{1-x-y}Ge_xC_y$/ p^- Si structures to determine ΔE_v of $Si_{1-x-y}Ge_xC_y$/ Si.

Figure 7 shows the band diagram of the p^+ $Si_{1-x-y}Ge_xC_y$ / p^- Si HIP structure. Under a reverse bias, hole current is mostly blocked by the valence band offset and the ideal leakage current comes from thermionically emitted holes from p^+ $Si_{1-x-y}Ge_xC_y$ layer. When an infrared light is incident on the p^+ $Si_{1-x-y}Ge_xC_y$ layer, holes will be excited to higher energy states, and if the photon energy is large enough for hole to overcome the barrier posed by the valence band offset, a photocurrent will result. From the band diagram, ΔE_V can be expressed as

$$\Delta E_v = E_{F(SiGeC)} + qV_{bi} + E_{F(Si)} \qquad (1)$$

where $E_{F(SiGeC)}$ is the distance between Fermi level and the valence band of $Si_{1-x-y}Ge_xC_y$, qV_{bi} is the built-in voltage of the junction, $E_{F(Si)}$ is the distance of the valence band of Si and the Fermi level. Since the $Si_{1-x-y}Ge_xC_y$ is heavily doped, the threshold energy for the onset of photocurrent is $E_v - E_{F(SiGeC)}$. To extract ΔE_v, one also needs to know the doping concentrations in $Si_{1-x-y}Ge_xC_y$ to calculate $E_{F(SiGeC)}$. Doping concentrations were obtained by SIMS measurement on similarly grown samples and SIMS data show no

dependence of dopant (boron) incorporation on the carbon level. We assume the onset current will track accurately with ΔE_V.

Figure 8 shows plots of the square root of photoresponse curves as a function of photon energy (Fowler plot) of $Si_{1-x-y}Ge_xC_y/Si$ with different carbon concentrations. The onset of photocurrent decreases as carbon level increases, indicating a decreasing ΔE_V with carbon concentrations. Carbon decreases the ΔE_V of $Si_{1-x-y}Ge_xC_y$ / Si by 26 ± 1 meV/%C, as shown in figure 9. This is consistent with previously reported values measured by C-V in HIP and MOS [20] structures, and similar to the increase in bandgap with carbon. We conclude that the increase in bandgap is reflected in the valence band of $Si_{1-x-y}Ge_xC_y$, with very little or no change in the conduction band. Thus small ΔE_c in $Si_{1-x-y}Ge_xC_y$ /Si is expected as in $Si_{1-x}Ge_x$/Si.

Figure 10 shows the valence band offset of $Si_{1-x}Ge_x$/Si and $Si_{1-x-y}Ge_xC_y$/Si as a function of lattice mismatch and equivalent Ge levels for $Si_{1-x}Ge_x$ of the given strain. Adding carbon lowers ΔE_V of $Si_{1-x-y}Ge_xC_y$ /Si, carbon reduces the lattice mismatch at a faster rate than reducing ΔE_V, compared to that achieved by reducing Ge alone in $Si_{1-x}Ge_x$. For example, the valence band offset of $Si_{0.585}Ge_{0.39}C_{0.025}$ / Si is ~100 meV larger than that of an equally strained $Si_{0.82}Ge_{0.18}$/Si heterostructure. Figure 10 also predicts that, by extrapolating the dashed line to the vertical axis, a strain-free $Si_{.563}Ge_{.39}C_{.047}$/Si heterostructure will have ~ 200 meV valence band offset. Since the Ge content determined by X-ray, SIMS and PL agrees within 5%, the effect of uncertainty in Ge concentration on this extrapolation is not significant. Even though the effect of uncertainty in determining C level could be as high as 30%, depending on the Ge/C strain compensation ratio used, the strain effect due to C incorporation on ΔE_V is not affected. Note that figure 4 was plotted based on lattice mismatch with Si.

II.D. Discussion.

X-ray photoelectron spectroscopy (XPS) measurement on $Si_{1-x-y}Ge_xC_y$ /Si indicated no significant change in ΔE_v with C incorporation (accuracy limit ±30meV) [21]. While this is in conflict with our work, the large error bars on that approach make it not very reliable. Our error bars are an order of magnitude smaller. Admittance spectroscopy on $Si_{1-x-y}Ge_xC_y$/Si multi-quantum wells suggested a large effect by carbon (~ 80 meV/ %C) on *both* the conduction and valence band offset of $Si_{1-x-y}Ge_xC_y$ /Si [22]. This is in direct conflict with our results. This reported C effect would imply that, a $Si_{1-x-y}Ge_xC_y$/Si heterostructure with 24% Ge and 1% C has ΔE_v ~ 90meV, a magnitude not enough to allow a complete hole transfer in the modulation-doped $Si_{.75}Ge_{.24}C_{.01}$ two-dimensional gas. However, this prediction is inconsistent with the observed complete carrier transfer from a doped Si supply layer to a modulation doped $Si_{1-x-y}Ge_xC_y$ two-dimensional hole gas [23]. Further, band offset studies by admittance spectroscopy measure the temperature-dependent conductance of $Si_{1-x-y}Ge_xC_y$ quantum wells and assumes that the conductance scales ideally as exp(-$\Delta E_v/kT$), as for thermionic emission. However, small signal conductance, like leakage current, can be easily dominated by non-ideal defects

Our capacitance-Voltage (C-V) measurement, on the other hand, has demonstrated a clear downward trend of ΔE_v of $Si_{1-x-y}Ge_xC_y$ /Si by carbon incorporation with minimal scatter of data among devices, and is insensitive to non-ideal leakage current. These measurements indicated that the increase in bandgap by carbon is fully accommodated in the valence band, with ΔE_v to Si decreasing by 20-26 meV/% substitutional carbon for small carbon concentrations [7,24]. Our optical measurements are also completely consistent with the electrical measurements. Further, the optical measurements are independent of leakage current mechanisms. Our results are consistent with a brief report of a few offsets measured by the indirect method of C-V analysis of $Si_{1-x-y}Ge_xC_y$ based metal-oxide-semiconductor (MOS) structures [14]. Note that having nearly all of the effect of carbon appear in the valence band is very attractive from the point of view of infrared detectors, which are nearly

9

all based on valence-band offsets in the SiGe material system. These results imply that all of the effect of carbon is "useful" since the bandgap change it causes is all directly falls on the relevant band of interest.

III. Summary

In summary, we have studied the valence band offset of compressively strained pseudomorphic $Si_{1-x-y}Ge_xC_y$ /Si (100) by heterojunction internal photoemission. Carbon decreased the valence band offset of $Si_{1-x-y}Ge_xC_y$/Si by 26 ± 1 meV/% carbon. Combining this number with a previously reported similar increase in the bandgap caused by carbon, we conclude that the band structure of $Si_{1-x-y}Ge_xC_y$ /Si exhibits a large valence band offset and a negligible conduction band offset, similar to that of $Si_{1-x}Ge_x$/Si heterostructures. This not only provides the basic materials technology and physics for the infrared detectors, but demonstrates that the SiGeC material system is technologically attractive as well.

IV. References

1. K. Eberl, S.S. Iyer, S. Zollner, J.C. Tsang, and F.K. LeGous, *Appl. Phys. Lett* **60**, 3033 (1992).

2. J.L. Regolini, F. Gisbert, G. Dolino, and P. Boucaud, *Mat. Lett* **18**, 57 (1993).

3. H.J. Osten, H. Rücker, M. methfessel, E. Bugiel, S. Ruminov, and G. Lippert, *J. Cryst. Growth* **157**, 405 (1995).

4. P. Boucaud, C. Guedj, F. H. Julien, E. Finkman, S. Bodnar, and J.L. Regolini, *Thin Solid Films* **278**, 114 (1996).

5. J. Kolodzey, P. R. Berger, B.A. Orner, D. Hits, F. Chen, A. Khan, X. Shao, M.M. Waite, S. Ismat Shah, C.P. Swann, and K.M. Unruh, *J. Cryst. Growth* **157**, 386 (1995).

6. C.W. Liu, A. St. Amour, J.C. Sturm, Y.R.J. Lacroix, M.L.W. Thewalt, C.W. Magee, and D. Eaglesham, *J. Appl. Phys.* **80**, 3043 (1996).

7. C.L. Chang, A. St. Amour, and J.C. Sturm, *Appl. Phys. Lett* **70**, 1557 (1997).

8. K. Brunner K. Eberl, and W. Winter, *Phys. Rev. Lett.* **76**, 303, (1996).

9. F.D. Shepherd, Proc. SPIE **1735**, 20 (1992).

10. X. Xiao, J. C. Sturm, et al, IEEE Elec. Dev. Lett. **EDL-14**, 199 (1993).

11. J.R. Jimenez, X. Xiao, J.C. Sturm, and P.W. Pellegrini, Appl. Phys. Lett. **67**, 506 (1995).

12. J.R. Jimenez, X. Xiao, J.C. Sturm, P.W. Pellegrini, and M.M. Weeks, J. Appl. Phys. **75**, 5160 (1994).

13. A. St.Amour, C.W. Liu, J.C. Sturm, Y. Lacroix, and M.L.W. Thewalt, *Appl. Phys. Lett* **67**, 3915 (1995).

14. L.D. Lanzerotti, A. St.Amour, C.W. Liu, and J.C. Sturm, *Elec. Dev. Lett*, **17**, 334 (1996).

15. P.Boucaud, C. Francis, F. Julien, J. Lourtioz, D. Bouchier, S. Bodnar, B. Lambert, and J. Regolini,*Appl. Phys. Lett* **64**, 875(1994).

16. K. Brunner, W. Winter, and K. Eberl, *Appl. Phys. Lett* **69**, 1279 (1996).

17. J.L. Regolini, F. Gisbert, G. Dolino, and P. Boucaud, *Mat. Lett* **18**, 57 (1993)

18. C.L. Chang, A. St. Amour, L. Lanzerotti, And J.C. Sturm, *Mat. Res. Soc. Sym. Proc.* **402**, 437 (1995).

19. S. Forrest and O. Kim, *J. Appl. Phys*, 52, 5838 (1981).

20. K. Rim, S. Takagi, J.J. Welser, J.L. Hoyt, and J.F. Gibbons, Mat. Res. Soc. Sym. Proc., **379**, 327, (1995).

21. M. Kim, and H.J. Osten, *Appl. Phys. Lett* **70**, 2702 (1997).

22. B.L. Stein, E.T. Yu, E.T. Croke, A.T. Hunter, T. Laursen, A.E. Bair, J.W. Mayer, C.C. Ahn, *Appl. Phys. Lett.*, **70**, 3413 (1997).

23. C-L. Chang, S.P. Shukla, W. Pan, V. Venkataraman, J.C. Sturm, and M. Shayegan, "Effective mass measurement in two-dimensional hole gas in strained $Si_{1-x-y}Ge_xC_y/Si(100)$ modulation doped heterstructures," *Thin Solid Films* **321**, 51-54 (1998).

24. C.L.Chang, A. St. Amour, and J.C. Sturm, *IEDM Tech. Digest*, 257 (1996).

11

V. Students Supported:

Three students were supported in part by these grants (USAF F49620-95-1-0438 (AASERT) and USAF F19628-96-K-0003) are:

Louis Lanzerotti: Ph.D. 1998. Current employer IBM, Burlington, VT.

Malcolm Carroll: Ph.D. 2001. Current employer Lucent Technologies/Bell Labs, Murray Hill, NJ.

Chialin Chang (F19628-96-K-0003 only): Ph.D. 1998. Motorola, Austin, TX.

IV. Publications and Presentations supported by this grant.

1. C.C. Chang and J.C. Sturm, "Effect of carbon on the valence band offset of compressively-strained $Si_{1-x-y}Ge_xC_y/$ (100) Si heterojunctions," Appl. Phys. Lett. (**70**), 1557-1559 (1997).

2. C.W. Liu and J.C. Sturm, "Low-temperature CVD growth of β-SiC on (100) Si using methylsilane and device characteristics," J. Appl. Phys. **82**, 4558-4565 (1997).

3. M. Yang, J.C. Sturm, and J.Prevost, "Band alignments and strain field distributions of zero- and one-dimensional pseudomorphic semiconductor particles," Phys. Rev. B **56**, 1973-1980 (1997).

4. L.D. Lanzerotti, J.C. Sturm, E. Stach, R. Hull, T. Buyuklimanli, and C. Magee, "Suppression of boron transient enhanced diffusion in SiGe heterojunction bipolar transistors by carbon incorporation," Appl. Phys. Lett. **70**, 3125-3126 (1997).

5. (Invited) A. St. Amour, L.D. Lanzerotti, C.C. Chang, and J.C. Sturm, "Optical and electrical properties of $Si_{1-x-y}Ge_xC_y$ thin films and devices," Thin Sol. Films **294**, 112-117 (1997).

6. C.L. Chang, A. St. Amour, and J.C. Sturm, "The effect of carbon on the valence band offset of compressively strained $SI_{1-x-y}Ge_xC_y/$(100) Si heterojunctions," *Appl. Phys. Lett.* **70** (12), 1557-1559 (1997).

7. M.S. Carroll, C-L Chang, and J.C. Sturm "Complete suppression of boron transient-enhanced diffusion and oxidation-enhanced diffusion in silicon using localized substitutional carbon incorporation," *Appl. Phys. Lett.* **73**, 3695-3697 (1998).

8. (Invited) J.C. Sturm "Advanced column-IV epitaxial materials for silicon-based optoelectronics," *Bull. Mat. Res. Soc.*, 60-64 (April 1998).

9. C. L. Chang, L. P. Rokhinson, J. C. Sturm, "Direct optical measurement of the valence band offset of p^+ $Si_{1-x-y}Ge_xC_y$ /p^- Si(100) by heterojunction internal photoemission," Appl. Phys. Lett., 3568-2570 (1998).

10. C.L. Chang, A. St. Amour, L.D. Lanzerotti, and J.C. Sturm, "Growth and electrical performance of heterojunction p^+-$Si_{1-x-y}Ge_xC_y/p^-$-Si diodes, "Proc. Symp. Mat.Res. Soc. **402**, 437-442 (1995).

11. M. Yang and J.C. Sturm, "Strain field effects on bandgap and band alignment in pseudomorphic zero- and one-dimensional structures, Tech. Prog. Elec. Mat. Conf., 72 (1996).

12. L.D. Lanzerotti, J.C. Sturm, E. Stach, R. Hull, T. Buyuklimanli, and C. Magee, "Suppression of boron outdiffusion in SiGe HBT's by carbon incorporation, "Tech. Dig. Inter. Elec. Dev. Mtg, 249-252 (1996).

13. C.C. Chang, A. St. Amour, and J.C. Sturm, "Effect of carbon on the valence band offset of $Si_{1-x-y}Ge_xC_y$/Si heterojunction, "Tech. Dig. Inter. Elec. Dev. Mtg, 257-260 (1996).

14. (Invited) A. St. Amour, L. D. Lanzerotti, C. C. Chang, and J. C. Sturm, "Optical and elecrical properties of $Si_{1-x-y}Ge_xC_y$ thin films and devices, Proc. Symp. Europ. Mat. Res. Soc. (1996), and Thin Solid Films **294**, pp. 112-117 (1997).

15. M. Carroll, L.L. Lanzerotti, C.C. Chang, and J.C. Sturm, "Silicon epitaxial regrowth in RTCVD for passivation of reactive ion-etched Si/SiGe/Si microstructures," Tech. Prog. Elect. Mater. Conf., 16 (1997).

16. L.D. Lanzerotti, J.C. Sturm, E.A. Stach, R. Hull, T. Buyuklimanli, and C. Magee, "Suppression of boron outdiffusion in SiGe HBTS by carbon incorporation, "Proc. Symp. Mat. Res. Soc. **469**, 297-302 (1997).

17. M. Carroll, L.L. Lanzerotti, C.C. Chang, and J.C. Sturm, "Silicon epitaxial regrowth in RTCVD for passivation of reactive ion-etched Si/SiGe/Si microstructures," Tech. Prog. Elect. Mater. Conf., 16 (1997).

18. C.L. Chang, S. Shukla, V. Venkataraman, J.C. Sturm, and M. Shayegan, "Effective mass measurement in two-dimensional hole gas in strained $Si_{1-x-y}Ge_xC_y$/ (100) modulation doped heterostructures," Tech. Dig. 7th Inter. Symp. Silicon Molec. Beam Epitaxy, 45-46 (1997).

19. M.S. Carroll, L.D. Lanzerotti, and J.C. Sturm, "Quantitative measurement of reduction of boron diffusion by substitutional carbon incorporation," Proc. Symp. Mat. Res. Soc., **527**, 417-422(1998).

20. C-L. Chang, S.P. Shukla, W. Pan, V. Venkataraman, J.C. Sturm, and M. Shayegan, "Effective mass measurement in two-dimensional hole gas in strained $Si_{1-x-y}Ge_xC_y$/Si(100) modulation doped heterstructures," *Thin Solid Films* **321**, 51-54 (1998).

21. (Invited) J.C. Sturm, M. Yang, C.L. Chang, and M.S. Carroll, "Novel Applications of rapid thermal chemical vapor deposition for nanoscale MOSFET's," Proc. Symp. Mat. Res. Soc. **525**, 273-281 (1998).

22. C.L. Chang and J.C. Sturm, "Polycrystalline $Si_{1-x-y}Ge_xC_y$ for suppression of boron penetration in PMOS structures," Proc. Symp. Mat. Res. Soc. **525**, 213-218 (1998).

23. C.L. Chang, L.P. Rokhinson, and J.C. Sturm, "Direct optical measurement of the valence band offset of p^+ $Si_{1-x-y}Ge_xC_y$ /p^- Si(100) by heterojunction internal photoemission," Proc. Symp. Mat. Res. Soc. **533**, pp. 245-250 (1998).
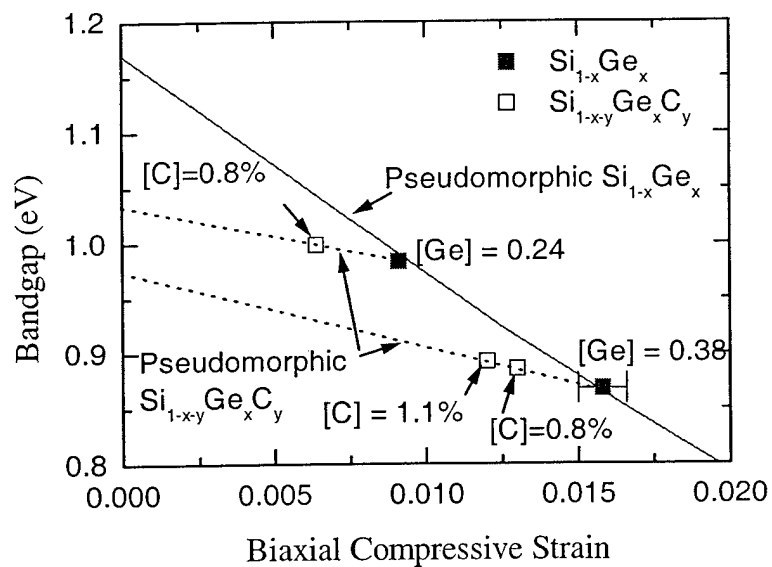
Fig. 1. Effect of SiGeC on lowering the biaxial compressive strain for a given bandgap vs. that for SiGe alloys commensurate on Si (100).
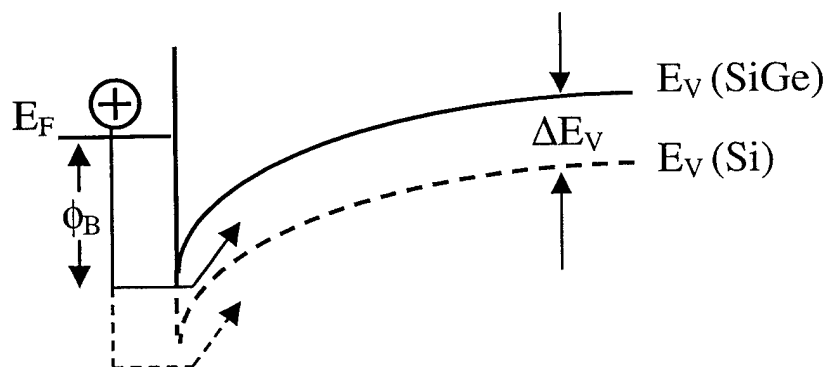

Fig. 2. Schematic diagram of hole barrier lowering in PtSi Schottky barrier detectors through the use of SiGe (or SiGeC) films on Si.
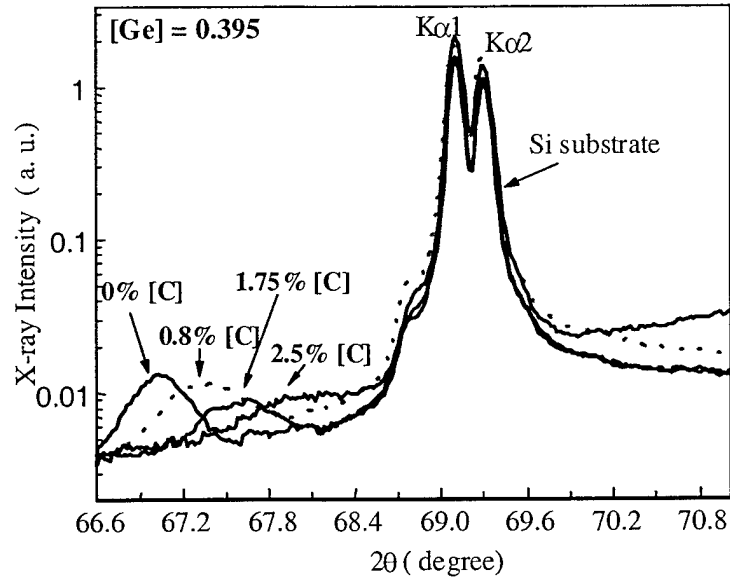
Fig. 3. (004) X-ray diffraction spectra for $Si_{1-x-y}Ge_xC_y$ thin films on Si (001). Two Si substrate peaks are due to Cu $K\alpha_1$ and $K\alpha_2$ x-ray lines. Broad $Si_{1-x-y}Ge_xC_y$ peaks are due to Scherer broadening in thin films.
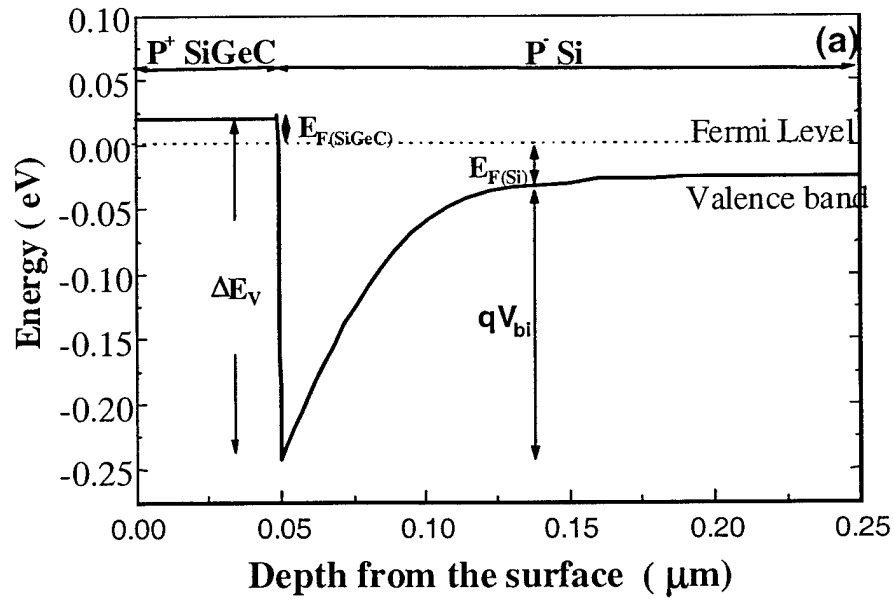
Fig. 4: Zero-bias valence Band diagram of p+ $Si_{1-x-y}Ge_xC_y$ / p⁻ Si diode.
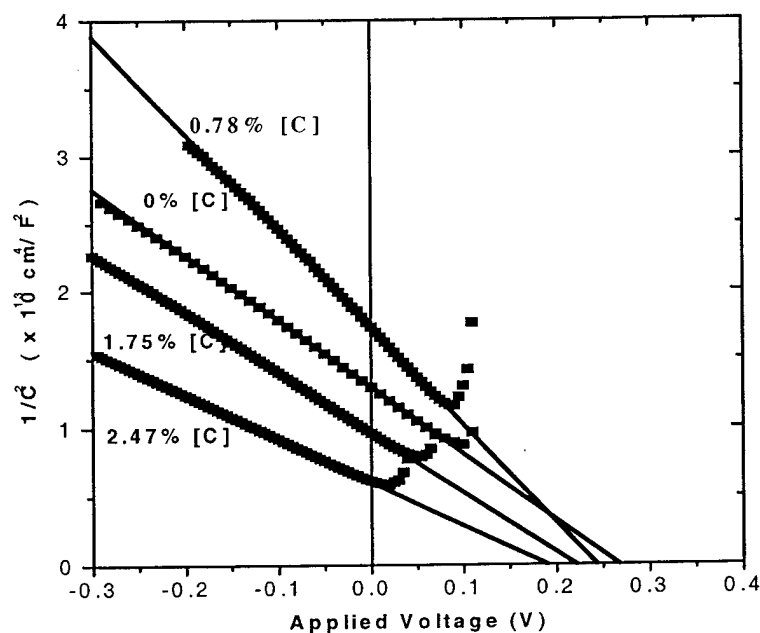
Fig. 5. $1/C^2$ is plotted against voltage for p^+ $Si_{1-x-y}Ge_xC_y$ / p^- Si with x=0.395 and different C concentrations.
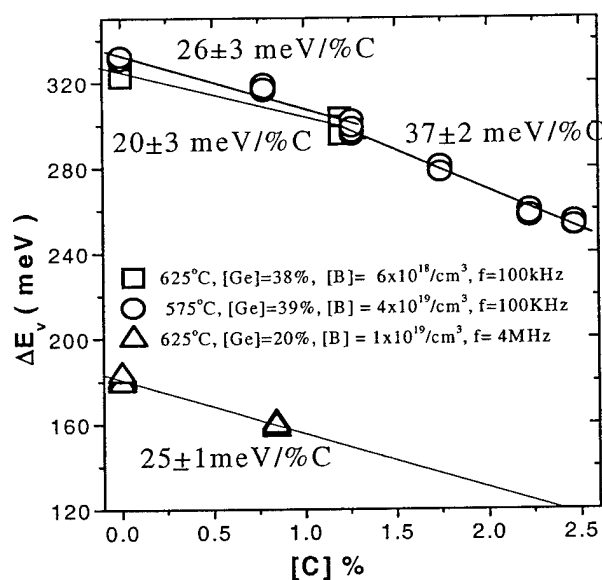

Fig. 6. $Si_{1-x-y}Ge_xC_y$ valence band offset to Si as a function of substitutional C content for different dopings, Ge concentration, and growth temperature. The lines are the best linear fits over the range of 0-1.3% C, and 1.3% - 2.5% C.
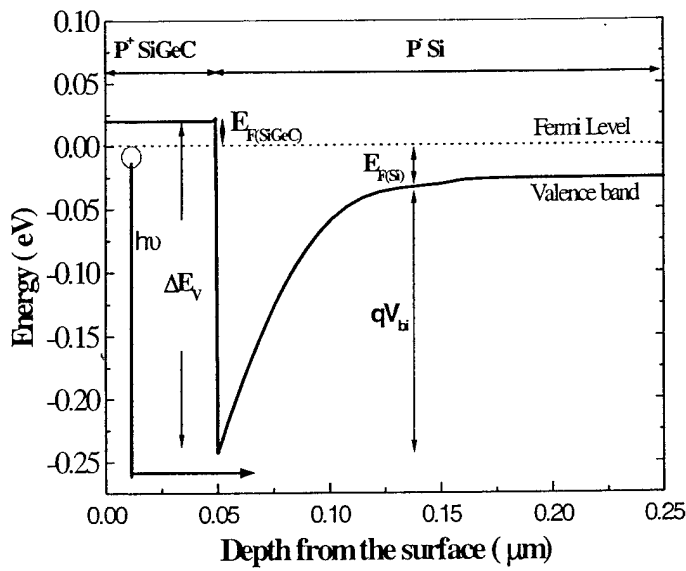
Figure 7: Zero-bias valence band diagram of p^+ $Si_{1-x-y}Ge_xC_y$ /p^- Si with optical excitation.

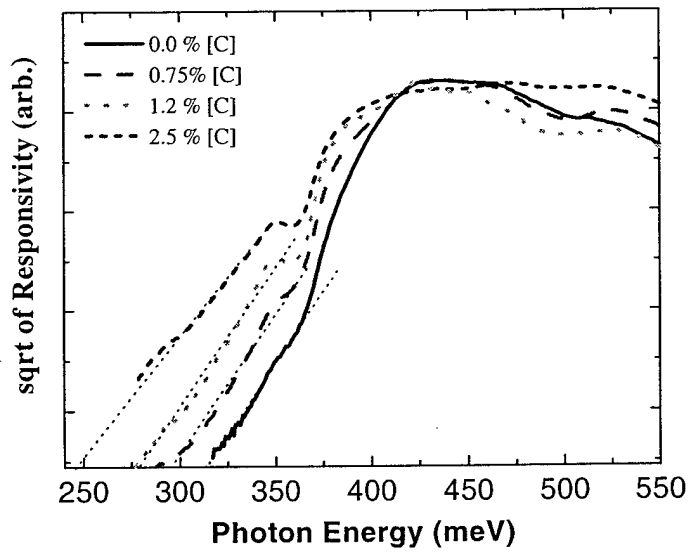Figure 8. Photoresponse curves of p^+ $Si_{1-x-y}Ge_xC_y$ /p^- Si as well as p^+ $Si_{1-x}Ge_x$/ p^- Si. Samples were measured at 4K.
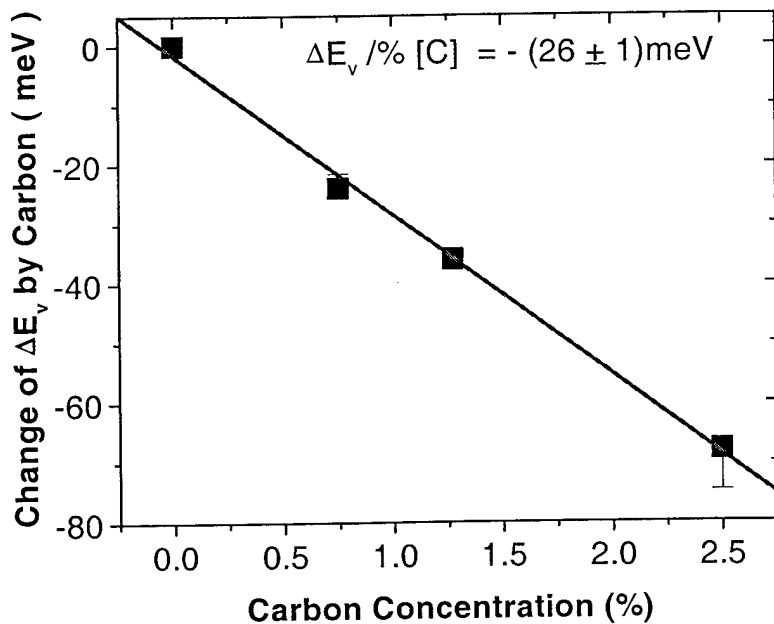
Figure 9. : Change of ΔE_v of $Si_{1-x-y}Ge_xC_y$ /Si as a function of C concentrations.
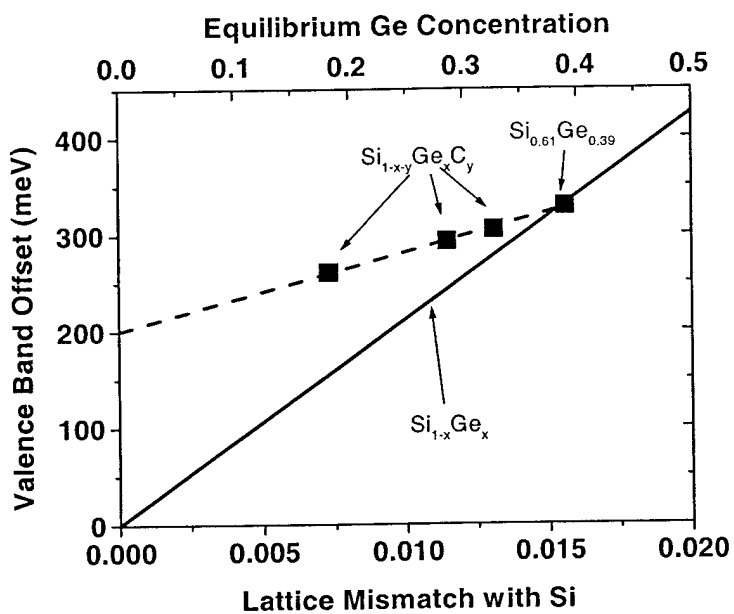

Figure 10: Summary of valence band offsets obtained from optical absorption measurement as a function of lattice mismatch with Si and equivalent Ge concentration. The solid line represents the valence band offsets of $Si_{1-x}Ge_x$/Si.